





# The RNA-binding protein Hfq is important for ribosome biogenesis and affects translation fidelity

José M Andrade<sup>1,†</sup> , Ricardo F dos Santos<sup>1,†</sup> , Irina Chelysheva<sup>2</sup>, Zoya Ignatova<sup>2,\*</sup>  & Cecília M Arraiano<sup>1,\*\*</sup> 

## Abstract

Ribosome biogenesis is a complex process involving multiple factors. Here, we show that the widely conserved RNA chaperone Hfq, which can regulate sRNA-mRNA basepairing, plays a critical role in rRNA processing and ribosome assembly in *Escherichia coli*. Hfq binds the 17S rRNA precursor and facilitates its correct processing and folding to mature 16S rRNA. Hfq assists ribosome assembly and associates with pre-30S particles but not with mature 70S ribosomes. Inactivation of Hfq strikingly decreases the pool of mature 70S ribosomes. The reduction in ribosome levels depends on residues located in the distal face of Hfq but not on residues found in the proximal and rim surfaces which govern interactions with the sRNAs. Our results indicate that Hfq-mediated regulation of ribosomes is independent of its function as sRNA-regulator. Furthermore, we observed that inactivation of Hfq compromises translation efficiency and fidelity, both features of aberrantly assembled ribosomes. Our work expands the functions of the Sm-like protein Hfq beyond its function in small RNA-mediated regulation and unveils a novel role of Hfq as crucial in ribosome biogenesis and translation.

**Keywords** Hfq; ribosome biogenesis; rRNA; translation

**Subject Categories** Microbiology, Virology & Host Pathogen Interaction; Protein Biosynthesis & Quality Control; RNA Biology

**DOI** 10.15252/embj.201797631 | Received 21 June 2017 | Revised 28 February 2018 | Accepted 13 March 2018 | Published online 18 April 2018

**The EMBO Journal (2018) 37: e97631**

See also: **IM Sharma et al** (June 2018)

## Introduction

Ribosomal RNA (rRNA) represents more than 80% of total RNA in the cell and along with a plethora of ribosomal proteins (r-proteins) constitutes the ribosome—the biosynthetic machinery of the cell. Ribosome biogenesis is a multi-step hierarchically ordered process in which processing of rRNA precursor (pre-rRNA) is a critical step. Emerging evidence suggests that pre-rRNA maturation serves as a

quality control to guarantee the integrity of the functional ribosome. In *Escherichia coli*, RNase III is responsible for the initial cleavages that separate individual rRNA precursors, followed by subsequent 5' and 3' processing by multiple ribonucleases to generate the 16S, 23S, and 5S rRNAs necessary to assemble the mature ribosomal subunits (Deutscher, 2009). Alterations in pre-rRNA processing cause conformational changes in the final rRNA and lead to aberrantly assembled immature ribosomal particles with largely compromised translational accuracy (Liiv & Remme, 2004; Roy-Chaudhuri et al, 2010; Yang et al, 2014). A parallel can be drawn to eukaryotes in which rRNA maturation errors lead to the production of defective ribosomal subunits (Cole et al, 2009; Fujii et al, 2012; Karbstein, 2013).

In prokaryotes, the small 30S ribosomal subunit contains 16S rRNA whereas 23S and 5S rRNA are the major components of the large 50S ribosomal subunit. The two asymmetric subunits include numerous r-proteins and associate to form the functionally active 70S ribosome (Shajani et al, 2011). Many auxiliary ribosome biogenesis factors, including GTPases, rRNA modification enzymes, helicases, and other maturation factors, assist rRNA folding and r-protein assembly pathway (Davis & Williamson, 2017). Strikingly, mutations affecting many of these accessory proteins cause dysfunctional ribosomes. In humans, such mutations were shown to lead to severe diseases, collectively referred to as ribosomopathies (Narla & Ebert, 2010).

The bacterial RNA-binding protein Hfq is a member of the Sm/Lsm superfamily of proteins with homologues in all domains of life (Wilusz & Wilusz, 2013). Hfq is an RNA chaperone which facilitates basepairing between small regulatory RNAs (sRNAs) and their mRNA targets. Consequently, Hfq controls the expression of many mRNAs either positively or negatively (Vogel & Luisi, 2011; Hajnsdorf & Boni, 2012; Updegrave et al, 2016). Importantly, in many bacteria, Hfq is not required for the sRNA-dependent pathways (Christiansen et al, 2006; Rochat et al, 2015), suggesting other yet undefined function(s) of Hfq beyond regulation of sRNA activity.

Hfq interacts *in vitro* with the 16S rRNA (de Haseth & Uhlenbeck, 1980) although the functional role of this interaction has remained elusive. Furthermore, rRNA molecules are commonly found in Hfq-enriched co-immunoprecipitations, what is usually regarded as

1 Instituto de Tecnologia Química e Biológica António Xavier, Universidade Nova de Lisboa, Oeiras, Portugal

2 Institute of Biochemistry and Molecular Biology, University of Hamburg, Hamburg, Germany

\*Corresponding author. Tel: (+49) 40 42838 2332; E-mail: Zoya.Ignatova@chemie.uni-hamburg.de

\*\*Corresponding author. Tel: (+351) 214 469 547; E-mail: cecilia@itqb.unl.pt

†These authors contributed equally to this work.

a background noise in transcriptomic studies (Zhang *et al*, 2003; Sittka *et al*, 2008; Bilusic *et al*, 2014). A cross-linking-based study in *E. coli* suggests interactions of Hfq with rRNA *in vivo* (Tree *et al*, 2014). An interaction between Hfq and S12 protein of the 30S ribosomal subunit has been previously reported, yet lacking mechanistic details on its role (Strader *et al*, 2013). Clearly, Hfq interacts with rRNA but is this a functional or redundant interaction?

Here, we identify a novel role of Hfq in ribosome biogenesis. Inactivation of Hfq leads to accumulation of 17S rRNA and reduced levels of 70S ribosomes in *E. coli*. Using *in vivo* and *in vitro* approaches, including ribosome profiling, we demonstrate that Hfq deletion affects the ribosome pool with direct effects on translation efficiency and fidelity. Our data propose Hfq as a novel auxiliary ribosome biogenesis factor. This expands the functional spectrum of this RNA chaperone beyond the sRNA-biology with impact on rRNA processing, ribosome biogenesis, and translation fidelity.

## Results

### Hfq is required for 16S rRNA maturation

The 16S rRNA arises from processing of the 17S rRNA precursor which harbors additional nucleotides (nts) at both extremities (Fig 1A). Hfq is a key regulator of cell physiology affecting gene expression in both exponential and stationary phases (Tsui *et al*, 1994; Muffler *et al*, 1997; De Lay *et al*, 2013). Thus, we compared the total RNA from wild-type and  $\Delta hfq$  cells extracted from exponential and stationary phase cells by Northern blotting using specific probes complementary to 5'- or 3'-ends of the 17S rRNA. In addition, we used probes corresponding to the internal regions of 16S rRNA or 23S rRNA (Fig 1B). Both 17S-specific probes hybridized only to 17S rRNA, whereas the 16S-probe identified both 16S and 17S rRNA. Notably, inactivation of Hfq in both growth phases resulted in higher levels of 17S rRNA with misprocessed extremities (28 and 148% increase in exponential and stationary phases, respectively), suggesting a role for Hfq in 16S rRNA maturation. On the other hand, Hfq did not significantly change the levels of 23S rRNA. The accumulation of 17S in the  $\Delta hfq$  mutant compared to the wild-type strain is observed over time in different points of the growth curve (Fig EV1A).

Hfq preferentially binds to the (ARN)<sub>x</sub> motif in RNAs (Mikulecky *et al*, 2004; Link *et al*, 2009; Peng *et al*, 2014). Strikingly, both 5' and 3' extremities of the 17S rRNA carry several of these predicted Hfq-binding sequences (Fig EV1B). To further assess the Hfq binding to these regions, we performed gel mobility shift experiments with constant amounts of the 5'-end and 3'-end sequences of 17S RNA and increasing levels of the Hfq protein (Fig 1C). Indeed, Hfq complexed with both 17S-end sequences corroborating the idea that Hfq interacts *in vitro* with 17S rRNA specific sequences.

The additional nucleotides from the 17S rRNA could interact with helix 1 and helix 2 of the mature 16S rRNA inducing alternative structures which would affect the folding of the central pseudoknot (Lodmell & Dahlberg, 1997; Roy-Chaudhuri *et al*, 2010). To evaluate whether the deletion of Hfq leads to an altered conformation of the 16S rRNA, we performed RNA mapping using two chemical probes, dimethyl sulfate (DMS) and *N*-cyclohexyl-*N'*-(2-morpholinoethyl)

carbodiimide (CMCT), in separate experiments (Fig 1D). A specific antisense primer to the 5'-end of the 16S rRNA was used in the primer extension reactions which allowed good resolution of the 16S central pseudoknot that consists of helix 1 (nucleotides 9–13/21–25) and helix 2 (nucleotides 17–19/916–918; Brink *et al*, 1993). Several nucleotides accessible to DMS (adenosines and cytidines) or CMCT (uridines and guanosines) modification in the wild type were less reactive to these probes in the absence of Hfq (Fig 1D). Our data imply that the folding of the 16S rRNA is altered as consequence of Hfq inactivation, resulting in the structural occlusion of those residues. Altogether, our observations indicate that Hfq interacts with 17S rRNA and is necessary for the correct processing and folding of the mature 16S rRNA, and affects the formation of the central pseudoknot.

### Inactivation of Hfq results in altered profiles of ribosome sedimentation

Given that misprocessing of rRNA can be consequence of defects in ribosome assembly (Liiv & Remme, 2004; Roy-Chaudhuri *et al*, 2010; Shajani *et al*, 2011), we next examined whether the defects in the maturation of 16S rRNA found in the  $\Delta hfq$  strain had consequences to the total amount of ribosomes. We profiled the ribosomes from exponential and stationary phase cultures of wild-type and mutant  $\Delta hfq$  strains by sucrose gradient ultracentrifugation (Fig 2A and B). The ribosome identity in the different peaks was further confirmed by analyzing their rRNAs (Appendix Fig S1). In the wild-type strain, under conditions that favor ribosome association (10 mM Mg<sup>2+</sup>), the peak corresponding to the small 30S subunits was nearly absent, while the amount of the 70S ribosomes was comparable between exponential and stationary phases (Fig 2A and B, and Appendix Fig S1). In clear contrast, the levels of the mature 70S ribosomes were reduced in the  $\Delta hfq$  mutant as compared to the wild type, an effect particularly severe in the stationary phase. Additionally, free 30S accumulated in the  $\Delta hfq$ , which again was more evident in stationary phase (Fig 2A and B). The complementation of the  $\Delta hfq$  deletion *in trans* with a plasmid expressing Hfq (pHfq; Andrade *et al*, 2012) raised the amount of mature ribosomes to levels comparable to that of the wild-type strain (Fig 2A and B, Appendix Fig S1). Strikingly, the plasmid expressing Hfq rescued the defects in the ribosomal amounts isolated from the Hfq deletion strain. Note that the  $\Delta hfq$  strain transformed with the empty vector was essentially identical to the  $\Delta hfq$  strain suggesting no effects of the transformation itself.

Our data clearly demonstrate that the inactivation of Hfq leads to a reduction in the pool of 70S ribosomes in the cell. This could either result from imbalanced production of subunits or the occurrence of major defects in the assembly of the 70S particle upon inactivation of Hfq. To distinguish between these two possibilities, we further analyzed ribosomes under dissociative conditions (0.1 mM Mg<sup>2+</sup>) to guarantee that all ribosomal subunits would be in their free state. As observed in Fig 2A and B (right panels), both strains displayed comparable contents of 30S and 50S subunits irrespective of the growth phase. Hence, the lower levels of 70S ribosomes in the absence of Hfq (Fig 2A and B, left panels) are a consequence of defects in the 70S assembly.

A well-known hallmark of ribosome biogenesis defects in bacteria is the cold-sensitive phenotype (Connolly & Culver,

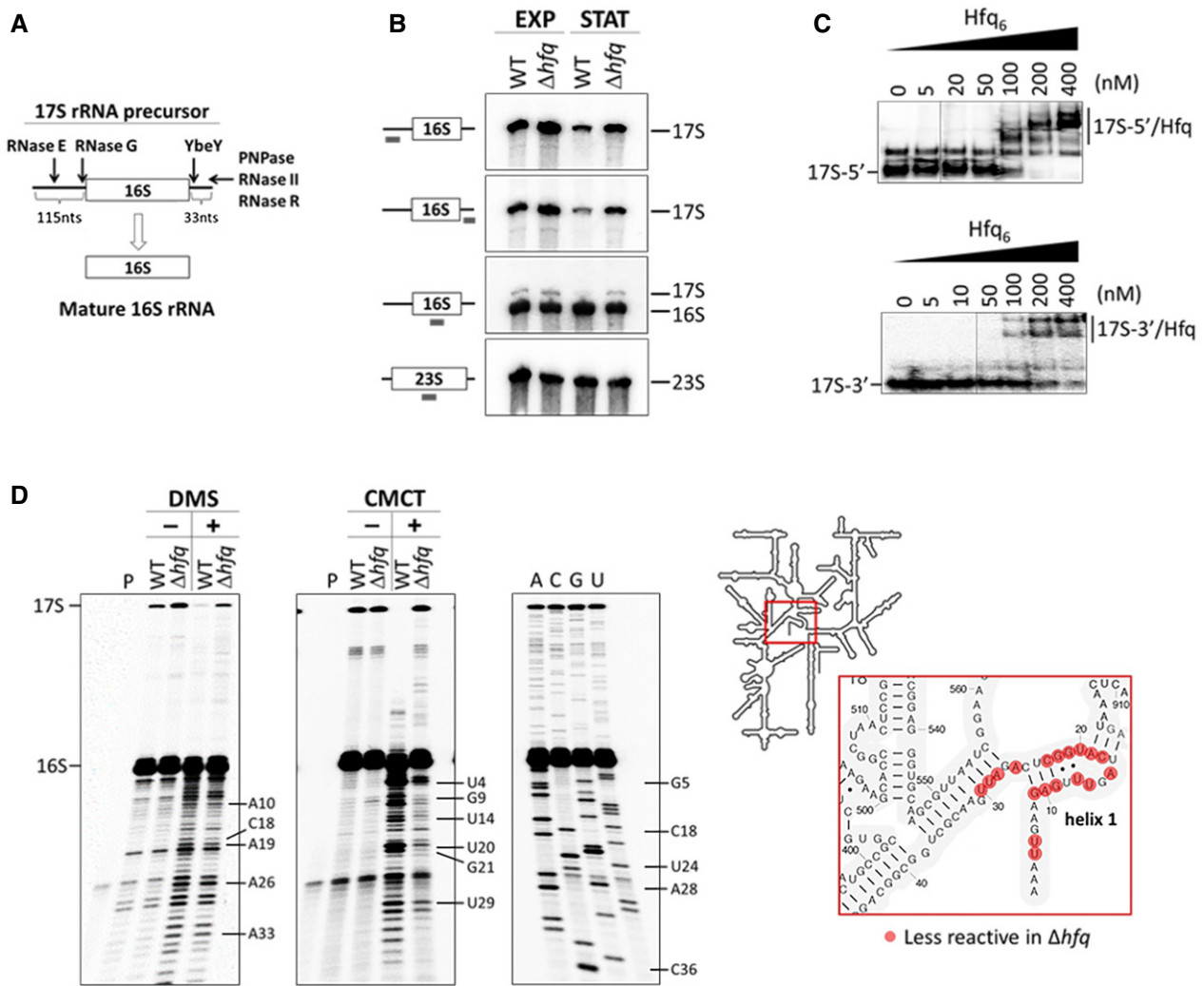


**Figure 1. Hfq is required for correct processing and folding of 16S rRNA.**

**A** Schematic representation of the RNase-mediated processing of the 17S rRNA precursor into mature 16S rRNA.  
**B** Northern blot analysis of total RNA extracted from cells in exponential (EXP) or stationary (STAT) growth phase. Samples were fractionated on a 4% polyacrylamide/7 M urea gel. A scheme of the probes binding to the rRNA sequence is displayed on the side.  
**C** Electrophoretic mobility shift assays of Hfq binding to the 5' and 3' extremities of the 17S rRNA. Increasing amounts of Hfq hexamer were mixed with a constant amount of the specific 17S-flanking sequences and resolved on a 6% (top panel) or 8% (bottom panel) native polyacrylamide gel.  
**D** DMS and CMCT accessibility probing of the 16S rRNA. Reverse-transcribed cDNA was fractionated on a 10% polyacrylamide/7 M urea gel. Residues with altered reactivities in the  $\Delta hfq$  mutant are indicated. The inset depicts the analyzed region of the 16S rRNA.

Source data are available online for this figure.

2009). We next compared the growth of the wild-type and  $\Delta hfq$  strains at 37 and 16°C (Fig 2C). Clearly, the  $\Delta hfq$  mutant exhibited the cold-sensitive phenotype, with severe growth defects under cold shock but not at 37°C which correlated with the altered ribosome profile found in the absence of Hfq. This effect is reminiscent of the cold-sensitive phenotype observed with different ribosome biogenesis factors like RbfA, KsgA, RimM, and RimO (Bylund et al, 1998; Connolly et al, 2008; Leong et al, 2013).

rRNA synthesis feedforwards the synthesis of ribosomal proteins (Scott et al, 2014). Thus, to assess the expression of the r-proteins, we used ribosome profiling which captures the

positions of actively translating ribosomes and the ribosome-protected fragments (RPFs) reporting on differences in gene expression at the level of translation (Ingolia et al, 2009; Li et al, 2014). This analysis was combined with RNA-Seq to determine the mRNA expression levels and the regulation of gene expression at the level of transcription. Strikingly, all ribosomal proteins were significantly translationally downregulated in the  $\Delta hfq$  mutant strain while the levels of their transcripts remained unchanged or decreased to much lower extent (Figs 2D and EV2A, and Dataset EV1). Notably, among the significantly enriched gene ontology (GO) terms are genes participating in ribosome assembly (Dataset EV1). Furthermore, within the polycistronic mRNAs, the

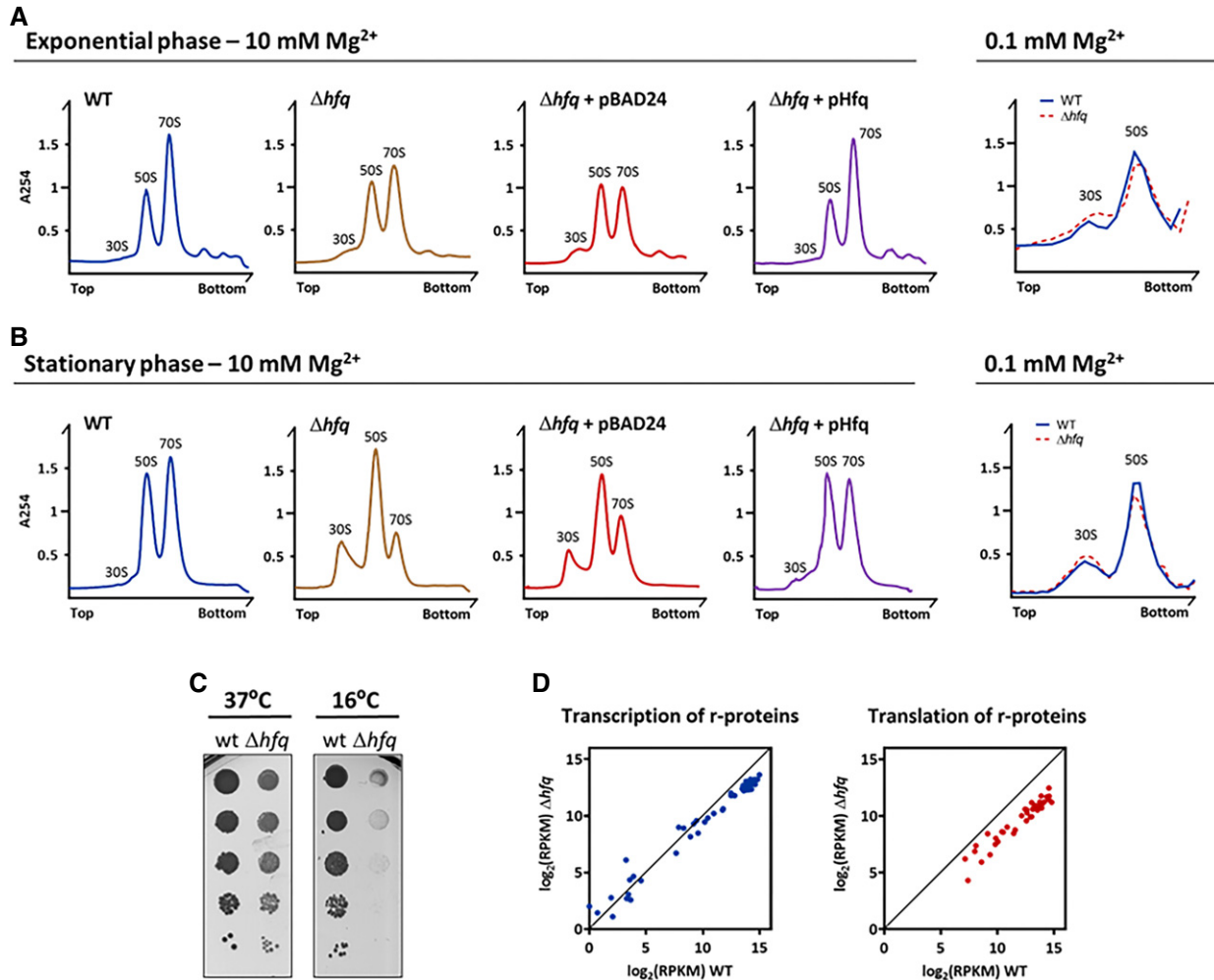


**Figure 2. Defective ribosome biogenesis in the  $\Delta hfq$  strain.**

A, B (Left panels) Ribosomes from cells in the exponential or stationary phase were fractionated on sucrose density gradients in 10 mM Mg<sup>2+</sup> to stabilize 70S particles with and without *trans*-complementation of *hfq* gene using pBAD24 plasmid. Ribosome species are identified over each peak; top and bottom denote the lowest (15%) and highest (45%) sucrose concentration in the gradient, respectively. (Right panels) Ribosomes purified from cells in exponential and stationary phases fractionated on sucrose density gradients at low 0.1 mM Mg<sup>2+</sup> concentration to promote 70S dissociation into free 30S and 50S subunits. Top and bottom denote the lowest (10%) and highest (30%) sucrose concentration in the gradient, respectively.

C Serial dilutions (with 1:1.10 steps) of wild-type and  $\Delta hfq$  strains grown on LB-agar plates at 37 or 16°C.

D Comparison of mRNA expression (left) and protein production (right) of ribosomal proteins between wild-type and  $\Delta hfq$  strains analyzed by RNA-Seq (left) and ribosome profiling (right), respectively.

Source data are available online for this figure.

translation yields of the encoded r-proteins differed (Fig EV2B and Dataset EV1) implying an independent translation initiation of the r-proteins (Li *et al.*, 2014). This expression pattern corroborates earlier observations for translational coupling of the expression of the ribosomal proteins and rRNA synthesis (Jinks-Robertson & Nomura, 1981; Nomura, 1999). Cumulative profiles of all expressed genes do not differ between wild-type and  $\Delta hfq$  strains, arguing against an effect of Hfq depletion on translation initiation (Fig EV3A).

Overall, our results show that the Hfq depletion leads to defects in ribosome biogenesis with consequences for the pool of mature 70S ribosomes and propose Hfq as an auxiliary factor which regulates ribosome biogenesis.

### Hfq copurifies with immature 30S subunits

We hypothesized that Hfq would preferably bind to immature 30S subunits as these can be enriched in 17S RNA. To test this, we purified immature 30S subunits from the knockout mutant of RbfA, a late assembly factor that accumulates pre-30S particles enriched in 17S rRNA (Jones & Inouye, 1996; Bylund *et al.*, 1998; Thurlow *et al.*, 2016). Compared to the wild-type, the  $\Delta rbfA$  mutant showed a similar ribosome profile to the  $\Delta hfq$  mutant, with increasing levels 30S particles and lower levels 70S ribosomes (Fig 3A). The peak corresponding to the 30S fraction was recovered from the sucrose gradients of the  $\Delta rbfA$  mutant, and the 30S subunits were purified in low salt conditions. In parallel, mature 30S subunits were

obtained from dissociation of 70S ribosomes isolated from the wild type, also in low salt conditions. Purified 30S samples were then analyzed by mass spectrometry that identified proteins associated with 30S subunits. Most of the proteins identified corresponded to r-proteins or known factors associated with ribosomes (Dataset EV2). Strikingly, Hfq was found to copurify only with immature 30S isolated from the  $\Delta rbfA$  but not with the mature 30S isolated from the wild type (Fig 3B). The same 30S samples were analyzed by Western blotting using an anti-Hfq antibody. Cell lysates of wild-type and  $\Delta hfq$  strains and purified His-tagged Hfq were used as controls. Western blot confirmed the presence of Hfq in the 30S purified from the  $\Delta rbfA$  but not from the wild type, in total agreement with mass spectrometry data (Fig 3C). Overall, these results show that Hfq is copurifying with precursor 30S ribosomes *in vivo* and corroborates that Hfq is a novel factor that assists ribosome assembly.

### Hfq affects translation efficiency

Altered ribosome biogenesis can lead to major defects in translation, and thus, we next assessed the translational status in the  $\Delta hfq$  mutant. Firstly, the  $\Delta hfq$  strain showed a reduced polysome fraction compared to that of the wild-type strain (Fig 4A). Secondly, a global measurement of protein synthesis by pulse metabolic labeling confirmed a significant reduction of translation in Hfq-depleted background (Fig 4B). Thirdly, the global translation efficiency, which was determined by the density of ribosomes from the ribosome profiling per mRNA from the RNA-Seq dataset, was significantly reduced (Mann–Whitney *U*-test or Wilcoxon rank-sum test,  $P = 0.0001996$ ; Fig 4C). Hence, the defects in rRNA precursor processing and ribosome biogenesis in the  $\Delta hfq$  mutant decreased translation volume and efficiency as compared to the parental strain. The well-known importance of Hfq for stress response in *E. coli* could arise from this effect on translational capacity, and not only from Hfq's role in sRNA-dependent regulation.

We next asked whether these changes in translation efficiency are global or a fraction of genes escapes this trend. We performed a fold-change analysis and ranked the genes according to the fold-change in translation (i.e., only translationally up- or downregulated in the ribosome profiling set) but with unchanged mRNA expression from the RNA-Seq experiment. Genes with changes in their RPF coverage higher than twofold were considered. The gene ontology (GO) analysis of the downregulated genes in Hfq-depleted background showed several pathways being affected but with a significant GO term enrichment in genes participating in ribosome biogenesis, translation, and amino acid metabolism (Fig 4D and Dataset EV1). The complete list of genes with the GO categories is summarized in Dataset EV1. For comparison, density plots of representative examples downregulated in the  $\Delta hfq$  mutant (Fig EV3B) or with unaltered translation (Fig EV3C) are included. Notably, inactivation of Hfq augmented the mRNA levels of genes known to be regulated by Hfq-dependent sRNAs, while their translation was only slightly affected (Dataset EV3).

### Hfq affects translation fidelity

The ribosomal tRNA accommodation site (A-site) is formed by helix 44 of the 16S rRNA of the 30S subunit. Three aminoglycoside

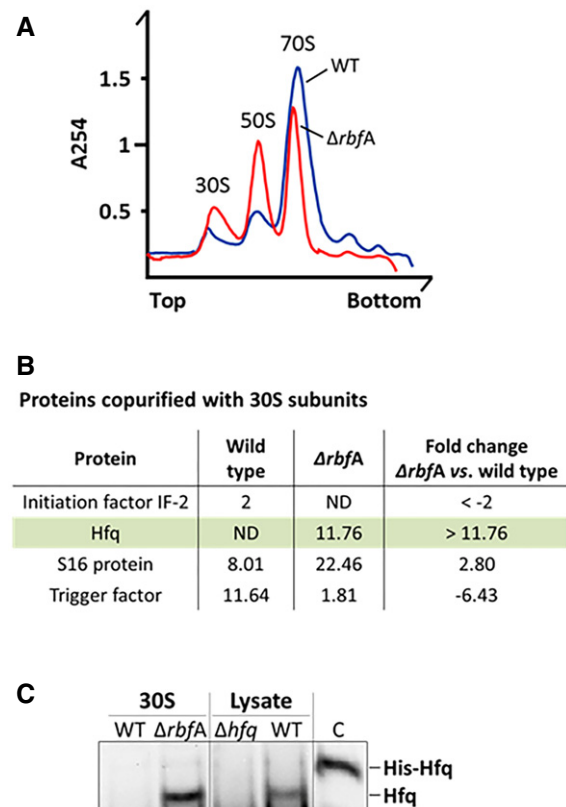


**Figure 3. Hfq copurifies with immature 30S subunits.**

- A** Ribosomes from wild-type and  $\Delta rbfA$  exponential growing cells were analyzed on sucrose density gradients. The  $\Delta rbfA$  mutant displays an altered ribosome profile with an increase in 30S and 50S subunits and a reduction of 70S ribosomes compared to the wild type.
- B** Representative proteins identified by mass spectrometry of purified 30S subunits from the wild-type and  $\Delta rbfA$  mutant. The measurement of all the peptides identified for each protein is shown as total ProtScore values calculated with the Pro Group™ Algorithm (Sciex), with a 95% confidence. The ratio between the  $\Delta rbfA$  mutant and wild type are shown as normalized fold changes that are represented by positive or negative values corresponding to an increase or decrease, respectively, of the number of peptides found in the  $\Delta rbfA$  mutant compared to the wild type. (ND, not detected).
- C** Western blot analysis of purified 30S subunits using an anti-Hfq antibody. WT and  $\Delta hfq$  cell lysates as well as purified His-Hfq protein were loaded as controls.

Source data are available online for this figure.

antibiotics, neomycin, paromomycin, and kanamycin, interact with the 16S rRNA near the A-site and induce translational misreading (i.e., shift of the reading frame, stop-codon readthrough; Foster & Champney, 2008). In the presence of sub-lethal concentrations of neomycin, paromomycin, or kanamycin, the  $\Delta hfq$  mutant strain showed exacerbated growth defects relative to untreated  $\Delta hfq$  or wild-type strains, suggesting that Hfq affects translation fidelity (Fig 5A). Additional aminoglycosides were further tested showing similar effect (Fig EV4). As control, the  $\Delta hfq$  strain did not show increased sensitivity to other classes of antibiotics, like colistin, which targets cell membrane (Figs 5A and EV4). We also investigated the misreading using a collection of widely used plasmids

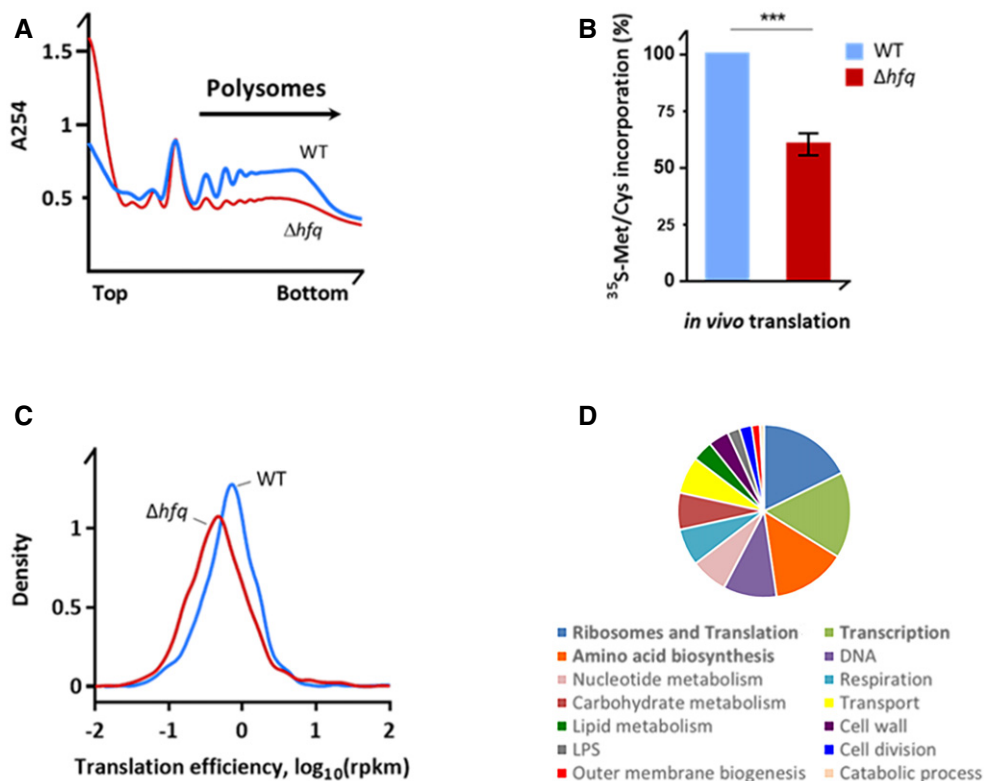


**Figure 4. The  $\Delta hfq$  strain displays reduced translation levels.**

- A Polysomal fraction is reduced in  $\Delta hfq$  cells. Polysome profiles of the wild-type and  $\Delta hfq$  strains were resolved on sucrose density gradient. Top and bottom denote the lowest (15%) and highest (50%) sucrose concentration in the gradient, respectively.
- B *In vivo* incorporation of  $^{35}\text{S}$ -methionine/cysteine translation assay in M9 medium. Data are normalized to the wild-type strain and are means  $\pm$  SEM ( $n = 3$ ). \*\*\* $p = 0.0004$  (paired *t*-test).
- C Translation efficiency of wild-type and Hfq-depleted cells obtained by ribosome profiling.
- D GO term analysis of translationally downregulated genes in the  $\Delta hfq$ . The top three affected categories are in bold. Full GO term analysis is included in Dataset EV1.

bearing *lacZ* as reporter (O'Connor *et al*, 1997). When compared with the isogenic parent, the  $\Delta hfq$  mutant showed a substantial increase in frameshifting, aberrant initiation from alternative start codon(s), and stop-codon readthrough (Fig 5B), indicating that the accuracy of translation in Hfq-depleted background is severely compromised. In sum, these data suggest that inactivation of Hfq decreases translation efficiency and enhances misreading of mRNA, implying a functional link between Hfq-dependent alterations in rRNA processing, ribosome biogenesis, and translation fidelity.

#### The distal face is critical for the Hfq-dependent regulation of ribosome biogenesis

The Sm-like Hfq assembles into a hexamer with a ring-like shape that displays at least three RNA-binding surfaces which confer Hfq the ability to bind simultaneously different RNA substrates. The proximal face and a charge patch in the outer rim of the hexamer bind preferably U-rich sRNAs while the distal face binds to A-rich sequences in target mRNAs (Mikulecky *et al*, 2004; Link *et al*, 2009; Otaka *et al*, 2011; Sauer & Weichenrieder, 2011; Sauer *et al*, 2012; Panja *et al*, 2013; Zhang *et al*, 2013).

To evaluate which binding surface would be responsible for the newly identified Hfq-dependent regulation of ribosome biogenesis, representative Hfq variants with mutations in the different surfaces (Zhang *et al*, 2013) were tested. Ribosome sedimentation profiles of proximal (Q8A and F39A), rim (R16A), and distal (Y25D and K31A) mutants isolated from exponential cultures were compared to that of the wild-type strain (Figs 6A and EV5). In addition, rRNAs from each fraction were isolated to confirm the ribosome identity in each peak (Appendix Fig S2). Strikingly, only mutations in the distal face caused reduction in the 70S ribosome levels, which were similar to those we observed for the Hfq deletion mutant (Fig 2A and B). The ribosome profiles of mutants in the proximal or rim surface were similar to that of the wild type, and these surfaces were shown to govern interactions with sRNAs (Sauer & Weichenrieder, 2011; Sauer *et al*, 2012; Panja *et al*, 2013; Zhang *et al*, 2013). Altogether, from these data, we conclude that the distal face of Hfq is critical for the regulation of the rRNA maturation and ribosome biogenesis and propose that the novel function of Hfq in the ribosome biogenesis might be independent of sRNA binding.

The sensitivity of the Hfq variant strains against different antibiotics was also tested (Fig 6B). The proximal and rim mutants (Q8A and R16A) did not show significant growth difference to the

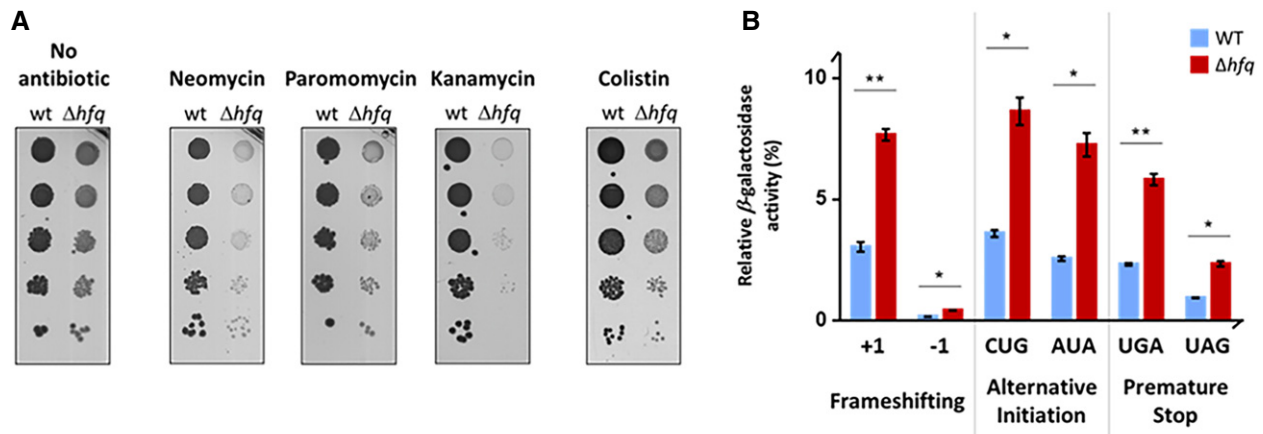


**Figure 5. Hfq-depleted cells exhibit increased codon misreading.**

A Serial dilutions (1:10) of wild-type and  $\Delta hfq$  strains grown on LB-agar plates at 37°C with and without sub-lethal concentrations of neomycin (1  $\mu$ g/ml), paromomycin (1  $\mu$ g/ml), kanamycin (1  $\mu$ g/ml), or colistin (0.1  $\mu$ g/ml).

B Wild-type and  $\Delta hfq$  strains expressing mutated *lacZ* gene (pSG plasmids) were tested for a frameshift mutation (+1 or -1), alternative initiation codons (CUG or AUA), or a non-sense stop-codon mutation (UGA or UAG). For each strain, the  $\beta$ -galactosidase activity (in Miller units) was normalized to that of strain expressing the wild-type *lacZ*. Data are means  $\pm$  SEM ( $n = 3$ ). \*\* $P < 0.01$ ; \* $P < 0.02$  (paired t-test).

Source data are available online for this figure.

wild type. Only the distal Hfq-Y25D variant showed increased susceptibility to aminoglycosides, like neomycin or kanamycin, suggesting that Hfq-Y25D is impaired in translation efficiency. However, the growth defect of Hfq-Y25D strain is not as severe as the one found in the knockout  $\Delta hfq$  mutant, which suggest that Y25D is an important residue but is not the sole responsible for the increased susceptibility to aminoglycosides. This phenotype was not observed when other classes of antibiotics were tested, such as polypeptide antimicrobials like colistin. These results from antibiotic sensitivity further support the importance of the distal face of Hfq in translation.

## Discussion

Here, we present results that support a novel role of Hfq in bacterial ribosome biogenesis with important consequences for translation (Fig 7). Hfq is a widely conserved RNA-binding protein of the Sm/Lsm family of proteins (Wilusz & Wilusz, 2013) that it is mostly known for promoting sRNA basepairing with target mRNAs (Updegrave *et al.*, 2016). However, a role of Hfq in regulating rRNA processing and folding has not been proposed. Our work unveils previously undescribed roles of Hfq in ribosome biogenesis and expands the repertoire of Hfq functions in the cell.

We show that Hfq is a new regulator of rRNA maturation. Hfq depletion results in loss of normal processing of rRNA, leading to the accumulation of unprocessed 17S rRNA precursor. Earlier cross-linking studies in *E. coli* identified interactions between Hfq and rRNA (Tree *et al.*, 2014), but did not analyze it further. We find that Hfq directly interacts with the 17S rRNA and Hfq inactivation results in the misprocessing of both 17S extremities. Our data align well with observations made for Lsm proteins, the evolutionarily conserved eukaryotic counterparts of the bacterial Hfq; depletion of Lsm proteins causes defects in the processing of pre-rRNAs (Kufel *et al.*, 2003; Beggs, 2005) supporting the notion for an evolutionary

conserved function of the members of the Sm/Lsm protein family in rRNA processing.

Accumulation of the 17S rRNA precursor is usually linked to problems in formation of mature 30S subunit, and most likely because maturation of 16S rRNA is a final step in ribosome biogenesis (Srivastava & Schlessinger, 1988; Shetty & Varshney, 2016). rRNA synthesis and maturation are tightly intertwined with the r-protein biosynthesis (Jinks-Robertson & Nomura, 1981; Nomura, 1999; Scott *et al.*, 2014). In the  $\Delta hfq$  background, accumulation of unprocessed 17S rRNA is accompanied with significant reduction of r-proteins synthesis, substantial reduction in the levels of 70S ribosomes, and concomitant accumulation of immature ribosomal subunits. The initiation of translation is the most sensitive node in translation regulation and defects during this process could lead to a similar phenotype (Laursen *et al.*, 2005). However, translation initiation remains unaffected upon Hfq inactivation (Fig EV3A). Along with the fact that *in trans*-complementation with Hfq rescues the defective ribosome assembly, we show that Hfq is needed for proper ribosome biogenesis but unessential for proper initiation. Hfq-depleted cells show phenotypes typically found in mutants of ribosome biogenesis factors, namely defects in rRNA maturation, accumulation of rRNAs precursors, and cold sensitivity (Kaczanowska & Rydén-Aulin, 2007; Shajani *et al.*, 2011). rRNA precursors compete with mature rRNAs for binding to r-proteins, although pre-rRNA containing ribosomes are conformationally defective (Liiv & Remme, 2004; Yang *et al.*, 2014).

Several auxiliary factors associate with the ribosome during the intricate process of ribosome assembly assisting in r-protein binding and rRNA folding steps (Kaczanowska & Rydén-Aulin, 2007). Hfq is a novel assembly factor that preferentially binds immature 30S subunits, like other chaperones such as RimM or RbfA. Like these factors, Hfq probably acts to facilitate or proofread folding of the pre-rRNA and pre-30S assembly. Hfq is a well-known RNA chaperone able to remodel RNA secondary structures (Moll *et al.*, 2003;

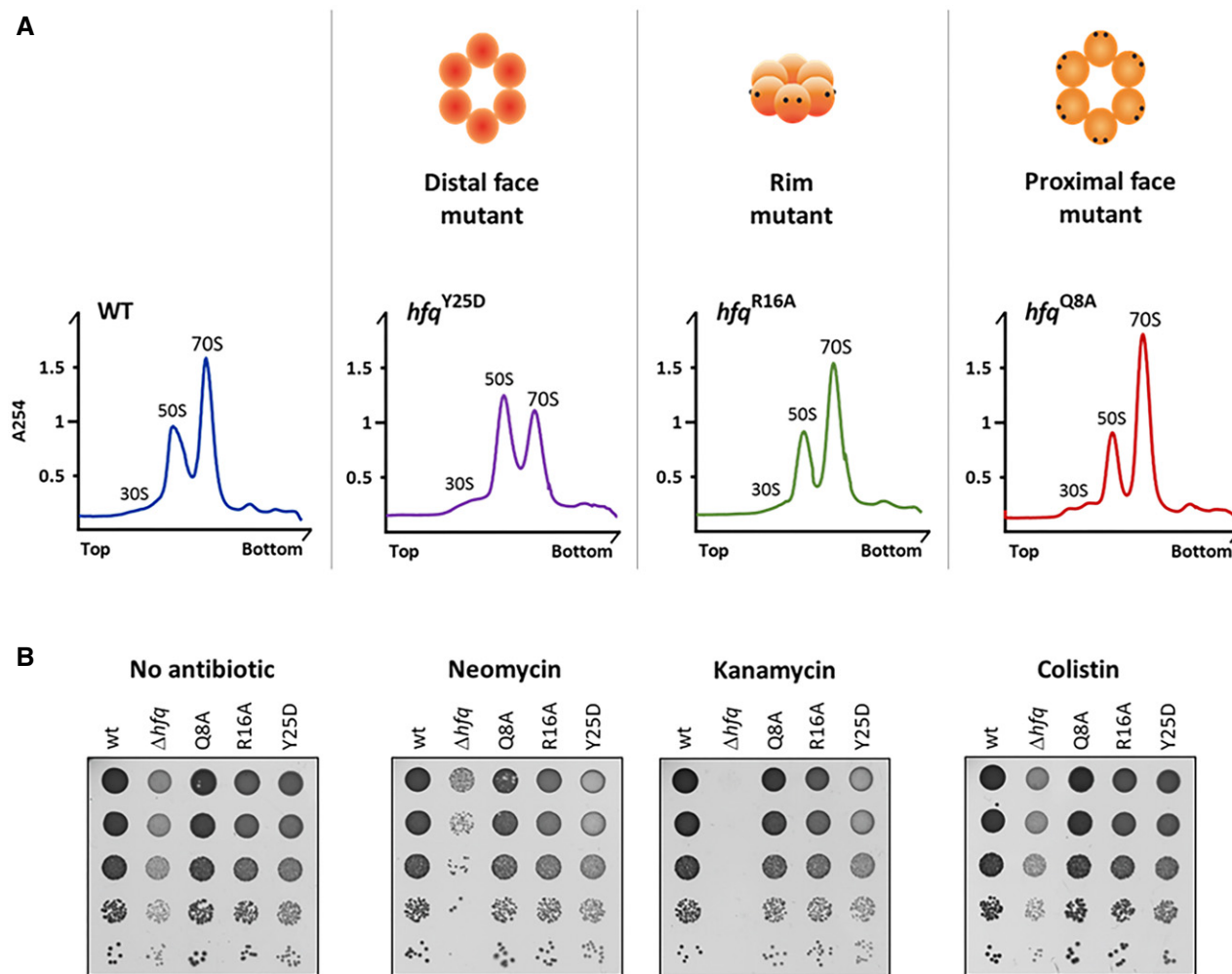


**Figure 6. The distal face of Hfq is required for correct ribosome biogenesis and translation fidelity.**

A Ribosomes purified from strains with specific point mutations in the *hfq* gene were fractionated on sucrose density gradients and compared to the wild-type strain. The binding surface affected by each mutation is schematically depicted on the top.

B Serial dilutions (1:10) of wild-type,  $\Delta$ *hfq*, and Hfq variants grown on LB-agar plates at 37°C with and without sub-lethal concentrations of neomycin (1  $\mu$ g/ml), kanamycin (1  $\mu$ g/ml), or colistin (0.1  $\mu$ g/ml).

Source data are available online for this figure.

Wroblewska & Olejniczak, 2016); hence, it is conceivable that it might be essential for the correct processing and folding of 16S rRNA into 30S subunits. In fact, cells lacking Hfq present an altered rRNA folding as suggested by our RNA-structure mapping. This is likely a consequence of the additional nucleotides from the 17S rRNA precursor which perturb the formation of helices 1 and 2 of the 16S rRNA (Lodmell & Dahlberg, 1997; Roy-Chaudhuri *et al*, 2010). This in turn affects the folding of the central pseudoknot, a universally conserved structural element that establish long-range interactions within the 16S rRNA and that is critical for the overall folding of the small subunit (Brink *et al*, 1993). Moreover, alterations in the secondary structure of the pseudoknot result in error-prone ribosomes (Lodmell & Dahlberg, 1997) as we observed in the  $\Delta$ *hfq* mutant. Alternatively, Hfq may promote RNA-protein interactions that are important for the correct rRNA processing. Notably, Hfq was previously shown to bind to the S12 protein of the 30S

small subunit in *E. coli* (Strader *et al*, 2013). The S12 protein is a key mediator of translation fidelity in both prokaryotes and eukaryotes and is positioned in helix 44 of the 16S rRNA that is known to form extensive contacts with the large subunit (Yusupov *et al*, 2001; Cukras *et al*, 2003). Association of Hfq with S12 is suggested to be important for the correct folding of 16S rRNA and formation of interface between ribosomal subunits and consequently the assembly of 70S ribosomes. Moreover, the sensitivity of the  $\Delta$ *hfq* strain to aminoglycosides and the cumulative translation errors induced by *hfq* deletion corroborate the observation that the conserved helix 44 of 16S rRNA maintains translation fidelity and serve as aminoglycoside target (Davis, 1987).

The role of Hfq in promoting the basepairing between regulatory small RNAs and their target mRNAs constitutes the most well-known function of this RNA-binding protein. An interesting feature of Hfq is that it is possible to uncouple its multiple functions by



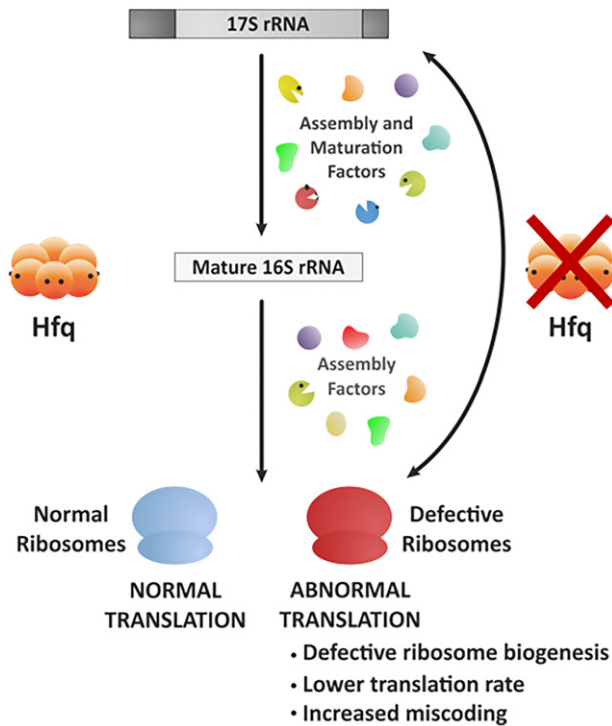


**Figure 7. Model for the Hfq regulation of ribosome biogenesis.**

Hfq assists ribosome biogenesis together with other ribosome assembly and maturation factors. Hfq depletion exhibits critical consequences for ribosome biogenesis and cellular translation. The  $\Delta hfq$  mutant affects the correct maturation of 30S subunits and accumulates unprocessed 17S rRNA precursor leading to a general translation deficiency.

introducing point mutations in each of its RNA-binding surfaces: the distal face of Hfq recognizes and binds to trinucleotide ARN repeats in mRNA, while the proximal and rim faces bind preferably to U-rich sequences in small RNAs (Link *et al*, 2009; Otaka *et al*, 2011; Sauer & Weichenrieder, 2011; Sauer *et al*, 2012; Panja *et al*, 2013). Strikingly, we found that the reduced levels of the 70S ribosomes in Hfq-depleted cells is dependent on residues located at the distal face of Hfq but not on those in the proximal and rim RNA-binding faces suggesting that rRNA regulation is independent of sRNA binding of Hfq. Despite Hfq being widely conserved, Hfq-dependent regulation of sRNAs is not a common feature; for example, this function is missing in many bacteria like *Bacillus subtilis* and *Listeria monocytogenes* (Christiansen *et al*, 2006; Rochat *et al*, 2015). Hfq is known to act independently of an sRNA as partner in a variety of cellular functions. Namely, Hfq stimulates the addition of poly(A) tails to the 3' end of mRNAs containing Rho-independent transcription terminators, promoting their degradation in *E. coli* (Le Derout *et al*, 2003; Mohanty *et al*, 2004; Folichon *et al*, 2005; Régnier & Hajnsdorf, 2013). Also, Hfq inhibits translation by binding directly to mRNAs, independent of a sRNA partner (Salvail *et al*, 2013; Ellis *et al*, 2015).

In summary, we have demonstrated that Hfq is a new ribosome assembly factor. Cells lacking Hfq exhibit diverse hallmarks of ribosome biogenesis defects, namely (i) misprocessing of rRNA and accumulation of 17S rRNA precursor; (ii) reduced pool of 70S ribosomes; (iii) an abnormal translation and compromised translation

fidelity; and (iv) cold-sensitive phenotype, typically associated with ribosome biogenesis factor mutants. This work expands the functions of Hfq beyond the regulation of small non-coding RNA biology and unveils unprecedented roles in ribosome biogenesis and translation.

## Materials and Methods

### Bacterial strains, plasmids, and oligonucleotides

All bacterial strains, plasmids, and oligonucleotides are listed in Appendix Tables S1–S3, respectively. All *E. coli* K-12 strains used in this study are derivatives of strains MG1693 or MC1061. Deletion of *hfq* was obtained using the  $\lambda$ -Red recombination (Datsenko & Wanner, 2000). The *hfq* point mutant alleles (Zhang *et al*, 2013) were P1-transduced to our parental strain, following selection on glucose minimal plates and screening for sensitivity to chloramphenicol. The  $\Delta rbfA$  mutant was obtained from the Keio collection (Baba *et al*, 2006). All mutations were confirmed by PCR and sequencing.

### Bacterial growth

Strains were grown in LB medium (Difco) supplemented with thymine (50  $\mu\text{g}/\text{ml}$ ) at 37°C, unless otherwise stated. Overnight cultures of single freshly grown colonies were diluted to an initial  $\text{OD}_{600} \sim 0.03$ . Cultures were collected either at exponential phase ( $\text{OD}_{600} \sim 0.5$ ) or stationary phase (after  $\sim 14$  h growth). Antibiotics were present at the following concentrations when needed: 25  $\mu\text{g}/\text{ml}$  chloramphenicol, 50  $\mu\text{g}/\text{ml}$  kanamycin, 10  $\mu\text{g}/\text{ml}$  tetracycline, and 100  $\mu\text{g}/\text{ml}$  ampicillin. For the dilution plating assays, serial dilutions were made in 10-fold increments and immediately spotted onto LB-agar plates. Sub-lethal concentrations of antibiotics were added when relevant: 1  $\mu\text{g}/\text{ml}$  neomycin, 1  $\mu\text{g}/\text{ml}$  paromomycin, 1  $\mu\text{g}/\text{ml}$  kanamycin, 0.1  $\mu\text{g}/\text{ml}$  colistin, 0.1  $\mu\text{g}/\text{ml}$  gentamicin, 1  $\mu\text{g}/\text{ml}$  streptomycin, 0.01  $\mu\text{g}/\text{ml}$  cefotaxime, 2  $\mu\text{g}/\text{ml}$  erythromycin, and 0.002  $\mu\text{g}/\text{ml}$  ciprofloxacin.

### RNA analysis

For Northern blots, total RNA was extracted as previously described (Andrade *et al*, 2012). One microgram of total RNA was resolved on 4% polyacrylamide/7 M urea gels in TBE 1 $\times$  buffer, transferred to a nylon membrane (GE Healthcare) and UV cross-linked. Membranes were hybridized with PerfectHyb Plus (Sigma-Aldrich) and probed with  $^{32}\text{P}$ -5'-end-labeled DNA oligonucleotides. Blots were analyzed on the Fuji TLA-5100 imaging system (GE Healthcare). RNAs collected from ribosome sedimentation fractions were extracted using TRI Reagent (Sigma-Aldrich) and resolved on agarose gels stained with ethidium bromide.

### Electrophoretic mobility shift assays

Binding assays were performed essentially as previously described (Andrade *et al*, 2013). The 17S rRNA extremities were generated by *in vitro* transcription with T7 RNAP (Promega) and [ $\alpha$ - $^{32}\text{P}$ ]-UTP (Perkin Elmer). EMSA samples were electrophoresed on native 6%

or 8% polyacrylamide gels in TBE 1× buffer in a cold room. Gels were exposed to a PhosphorImager screen (GE Healthcare).

### RNA mapping

Chemical modification reactions were carried out with DMS (diluted 1:6 in ethanol) or CMCT (1 mg/ml) following protocols described in Andrade *et al*, 2013 and Caprara, 2011; respectively. Total RNA (10 µg) extracted from exponential phase cultures ( $OD_{600} \sim 0.35$ – $0.40$ ) of wild-type and  $\Delta hfq$  strains was used. Primer extension reactions were carried out using the  $^{32}P$ -5'-end-labeled primer 46 (Clatterbuck Soper *et al*, 2013) and 100 U of reverse transcriptase SuperScript III or IV (Thermo Fisher Scientific). Samples were analyzed on 10% polyacrylamide/7 M urea gels run in TBE 1× buffer.

### Ribosome extraction and sucrose sedimentation

Ribosome isolation was adapted from (Powers & Noller, 1991). Cell pellets were resuspended in ice-cold buffer A (50 mM Tris–Cl at pH 7.5, 10 mM MgCl<sub>2</sub>, 100 mM NH<sub>4</sub>Cl, 0.5 mM EDTA, and 6 mM 2-mercaptoethanol) with the addition of Complete Mini Protease Inhibitor cocktail EDTA-free (Roche) and lysed by French press. After TurboDNase (Ambion) digestion, the clarified lysate was layered over a 36% sucrose cushion composed of buffer B (50 mM Tris–Cl at pH 7.5, 10 mM MgCl<sub>2</sub>, 500 mM NH<sub>4</sub>Cl, 0.5 mM EDTA, and 6 mM 2-mercaptoethanol) and spun at 120,000 g for 16 h in a Beckman ultracentrifuge 90Ti rotor at 4°C. The ribosome pellets were washed once with buffer C (50 mM Tris–Cl at pH 7.5, 10 mM MgCl<sub>2</sub>, 100 mM NH<sub>4</sub>Cl, and 6 mM 2-mercaptoethanol) and then resuspended in the same buffer by gentle rocking at 4°C. Purified ribosomes were analyzed in 15–50% (w/v) sucrose gradients prepared in buffer C with 10 mM MgCl<sub>2</sub> (associative conditions) or in 10–30% (w/v) sucrose gradients prepared in buffer C with 0.1 mM MgCl<sub>2</sub> (dissociative conditions). Associative samples were centrifuged in a Beckman ultracentrifuge SW41 rotor for 16 h at 71,000 g at 4°C and analyzed by UV using the AKTA system (GE Healthcare). Dissociative samples were centrifuged in a Beckman ultracentrifuge SW28 rotor for 16 h at 76,000 g at 4°C and fractions collected from the top were quantified on Nanodrop.

### Ribosome profiling, RNA-Seq, and data analysis

Ribosome-protected fragments and randomly fragmented mRNA for ribosome profiling and RNA-Seq, respectively, were isolated as described previously (Del Campo *et al*, 2015). Briefly, cells cultured to the exponential phase ( $OD_{600}$  0.35–0.40) in LB medium were split into two aliquots. From one aliquot, total RNA was extracted using TRI Reagent (Sigma-Aldrich), enriched by depleting small RNAs with GeneJET Purification Kit (Fermentas) and rRNA with MICROBExpress Bacterial mRNA Enrichment Kit (Ambion), and fragmented in alkaline solution (2 mM EDTA and 100 mM Na<sub>2</sub>CO<sub>3</sub> pH 9.2 for 40 min at 95°C) to fragments with size of 24–35 nts. The second aliquot was used to isolate mRNA-bound ribosome complexes. Cells were collected by filtration and flash-frozen without preincubation with antibiotics. Cells were lysed by freeze-rupturing (Retch Mill), and 100 A<sub>260</sub> units of ribosome-bound mRNA fraction were directly used for polysomal analysis or

subjected to nucleolytic digestion with 10 units/µl micrococcal nuclease (Fermentas) for 10 min at room temperature in buffer with pH 9.2 (10 mM Tris pH 11 containing 50 mM NH<sub>4</sub>Cl, 10 mM MgCl<sub>2</sub>, 0.2% Triton X-100, 100 µg/ml chloramphenicol, and 20 mM CaCl<sub>2</sub>) to obtain the monosomal fraction. Separation was obtained by sucrose density gradient (15–50% w/v). Subsequently, 20–35-nt RNA fragments from the monosomal fraction were size selected on a denaturing 15% polyacrylamide gel. For both ribosome-protected fragments and mRNA fragments, the libraries were prepared by direct ligation of the adaptors (Del Campo *et al*, 2015) and sequenced on the Illumina GAIIx platform. Sequenced reads were quality trimmed using *fastx-toolkit* (0.0.13.2; quality threshold: 20), and sequencing adapters were cut using *cutadapt* (1.8.3; minimal overlap: 1 nt) and mapped to the *E. coli* genome (strain MG1655, version U00096.3, NCBI) using Bowtie (1.1.2) allowing a maximum of two mismatches. The number of raw reads was used to generate gene read counts for each ORF, by counting the number of reads whose middle nucleotide (for even read length the nucleotide 5' of the mid-position) fell in the CDS. Gene read counts were normalized by the length of the unique CDS per kilobase (RPKM) and the total mapped reads per million (RPM; Mortazavi *et al*, 2008). Spike-ins (ERCC, Thermo, Germany) were added to the RNA-Seq data set upon rRNA depletion with MICROBExpress kit and used to set the detection threshold in each sequencing set. The same detection threshold was used for the corresponding ribosome profiling experiment. Furthermore, to determine the reproducibility of our sequencing data sets, we used published data set serving as a truly independent biological replicate in which bacteria were grown under identical conditions (GEO accession number, GSE85540; Hwang & Buskirk, 2017). The reproducibility is very high,  $R^2 = 0.865$  and  $R^2 = 0.816$  (Spearman correlation coefficient) for the RNA-Seq and ribosome profiling data sets, respectively. The correlation is even higher for the r-proteins only. For fold-change analysis, we used a threshold of 2. Cumulative profiles of read density for RPFs have been computed as described (Ingolia *et al*, 2009). The overlapping genes were excluded from this analysis as initiation of the downstream gene is within the open-reading frame of the upstream gene and the RPFs in this region cannot be unambiguously assigned to either gene. Gene ontology enrichment including statistical analysis was performed using the tools and gene lists from Gene Ontology Consortium (<http://geneontology.org/>).

### Analysis of purified 30S-associated proteins

For 30S purification, cells were grown in 1 l of LB medium at 37°C and 160 rpm agitation to an  $OD_{600} \sim 0.6$  for the wild-type strain and  $OD_{600} \sim 0.2$  in the case of the  $\Delta rbfA$  strain, as previously described with minor modifications (Thurlow *et al*, 2016). Ribosomes were isolated in a similar manner as detailed above. However, “low salt conditions” were used to allow mass spectrometry analysis, meaning that all buffers contained only 60 mM of NH<sub>4</sub>Cl. Isolated ribosomes were then quantified and separated on 15–45% (w/v) sucrose gradients under dissociative (0.1 mM MgCl<sub>2</sub>) and associative conditions (10 mM MgCl<sub>2</sub>) for the wild-type and  $\Delta rbfA$  strain, respectively. Gradients were centrifuged in a Beckman ultracentrifuge SW41 rotor at 71,000 g and 4°C for 16 h and analyzed by UV using the AKTA system (GE Healthcare). Fractions corresponding to 30S peak were collected and spun in a Beckman 90Ti rotor at

120,000 g and 4°C for 16 h to remove the sucrose buffer from the 30S particles. The pellet was then resuspended in buffer D (10 mM Tris-Cl at pH 7.5, 10 mM MgCl<sub>2</sub>, 60 mM NH<sub>4</sub>Cl, and 3 mM 2-mercaptoethanol) and stored at -80°C. Mature 30S subunits isolated from the wild-type strain and immature 30S particles isolated from the *ΔrbfA* strain were quantified on Nanodrop. Mass spectrometry data were obtained by the UniMS service (Mass Spectrometry Unit, ITQB/iBET, Oeiras, Portugal). Peptides were analyzed using the Pro Group™ Algorithm (Sciex), and for each protein, two types of scores were obtained: unused and total ProtScore. While the latter is a sum of the ion scores of all identified peptide evidence for a protein, the unused ProtScore reflects the amount of total unique peptide evidence related to the same protein. The confidence threshold was set at unused score of 2 and 1.3 with 99 and 95% confidence, respectively. A ratio from the *ΔrbfA* strain over the wild-type control was used to identify fold-change variation of proteins. Positive or negative fold-change values correspond to an increase or decrease, respectively, of the number of peptides found in the *ΔrbfA* mutant compared to the wild type. Hfq presence in purified 30S samples (2.5 μg) was further analyzed by Western blot using an anti-Hfq antibody (Ziolkowska *et al*, 2006).

#### Pulse-labeling assay

Bacteria were grown in M9 medium supplemented with 0.02% casaminoacids (Difco) in an orbital shaker at 37°C. Exponential phase cells were centrifuged, resuspended in M9 medium supplemented with 0.15 mM amino acid mix without methionine and cysteine (Promega), and incubated for 60 min in a water bath at 37°C. Labeling with <sup>35</sup>S-radiolabeled L-Met/L-Cys mix (Perkin Elmer) proceeded for 30 s at 37°C. Reaction was stopped with addition of TCA to a final concentration of 5%, and samples were spotted onto GF/C glass microfibers filters (Millipore). Filters were washed four times with TCA 5%, once with ethanol, and then dried under vacuum. <sup>35</sup>S signal on filters was quantified by scintillation counting using the Ready Safe Liquid Scintillation cocktail (Beckman Coulter).

#### β-Galactosidase assay

Translation fidelity was analyzed by measurement of the β-galactosidase activity using the pSG plasmid series (O'Connor *et al*, 1997). Cells were grown to log phase (OD<sub>600</sub> ~ 0.35–0.40) in LB medium at 37°C. β-galactosidase activity from the plasmid encoding WT *lacZ* was used for normalization in the respective set of MC1061 strains or MC1061 *Δhfq* mutant strains. Paired *t*-test statistical analysis performed using GraphPad Prism 6 software.

#### Statistical analysis and data deposition

The sequencing data were also submitted to GEO under the accession number GSE100373.

**Expanded View** for this article is available online.

#### Acknowledgements

We thank Susan Gottesman (National Cancer Institute, USA) and Eric Brown (McMaster University, Canada) for kindly providing strains. We are grateful to Sarah Woodson (Johns Hopkins University, USA) and Murray Deutscher

(University of Miami, USA) for insightful comments. We thank Ricardo Gomes (UniMS, ITQB NOVA/iBET, Portugal) for performing mass spectrometry services. Cristian del Campo is acknowledged for his help with the ribosome profiling protocol. This work was financially supported by Project LISBOA-01-0145-FEDER-007660 (Microbiologia Molecular, Estrutural e Celular) funded by FEDER through COMPETE2020—Programa Operacional Competitividade e Internacionalização (POCI) and by FCT—Fundação para a Ciência e a Tecnologia (Portugal), including project PTDC/BIA-MIC/1399/2014 to C.M.A., project PTDC/IMI-MIC/4463/2014 and FCT Investigator Programme (IF/00961/2014) to J.M.A.; European Union Horizon 2020 Research and Innovation Programme (grant agreement no. 635536) to C.M.A. and by the Deutsche Forschungsgemeinschaft (FOR1805) and European Union (grant NICHE ITN) to Z.I. R.F.d.S. is recipient of a FCT Doctoral fellowship (PD/BD/105733/2014) in frame of the ITQB PhD Program in Molecular Biosciences.

#### Author contributions

JMA conceived the project; JMA, ZI, and CMA designed experiments; JMA, RfDs, and IC performed experiments; all authors analyzed data; JMA, ZI, and CMA supervised the work; JMA and RfDs prepared the figures; JMA wrote the article, and all authors edited the manuscript.

#### Conflict of interest

The authors declare that they have no conflict of interest.

## References

- Andrade JM, Pobre V, Matos AM, Arraiano CM (2012) The crucial role of PNPase in the degradation of small RNAs that are not associated with Hfq. *RNA* 18: 844–855
- Andrade JM, Pobre V, Arraiano CM (2013) Small RNA modules confer different stabilities and interact differently with multiple targets. *PLoS One* 8: e52866
- Baba T, Ara T, Hasegawa M, Takai Y, Okumura Y, Baba M, Datsenko KA, Tomita M, Wanner BL, Mori H (2006) Construction of *Escherichia coli* K-12 in-frame, single-gene knockout mutants: the Keio collection. *Mol Syst Biol* 2: 2006.0008
- Beggs JD (2005) Lsm proteins and RNA processing. *Biochem Soc Trans* 33: 433–438
- Bilusic I, Popitsch N, Rescheneder P, Schroeder R, Lybecker M (2014) Revisiting the coding potential of the *E. coli* genome through Hfq co-immunoprecipitation. *RNA Biol* 11: 641–654
- Brink MF, Verbeet MP, de Boer HA (1993) Formation of the central pseudoknot in 16S rRNA is essential for initiation of translation. *EMBO J* 12: 3987–3996
- Bylund GO, Wipemo LC, Lundberg LA, Wikström PM (1998) RimM and RbfA are essential for efficient processing of 16S rRNA in *Escherichia coli*. *J Bacteriol* 180: 73–82
- Caprara M (2011) RNA structure determination using chemical and nuclease digestion methods. In *RNA: a laboratory manual*, Rio D, Hannon G, Ares M, Nilsen T (eds), pp 269–275. Cold Spring Harbor, NY: Cold Spring Harbor Laboratory Press
- Christiansen JK, Nielsen JS, Ebersbach T, Valentin-Hansen P, Sogaard-Andersen L, Kallipolitis BH (2006) Identification of small Hfq-binding RNAs in *Listeria monocytogenes*. *RNA* 12: 1383–1396
- Clatterbuck Soper SF, Dator RP, Limbach PA, Woodson SA (2013) *In vivo* X-ray footprinting of pre-30S ribosomes reveals chaperone-dependent remodeling of late assembly intermediates. *Mol Cell* 52: 506–516

- Cole SE, LaRiviere FJ, Merrikh CN, Moore MJ (2009) A convergence of rRNA and mRNA quality control pathways revealed by mechanistic analysis of nonfunctional rRNA decay. *Mol Cell* 34: 440–450
- Connolly K, Rife JP, Culver G (2008) Mechanistic insight into the ribosome biogenesis functions of the ancient protein KsgA. *Mol Microbiol* 70: 1062–1075
- Connolly K, Culver G (2009) Deconstructing ribosome construction. *Trends Biochem Sci* 34: 256–263
- Cukras AR, Southworth DR, Brunelle JL, Culver GM, Green R (2003) Ribosomal proteins S12 and S13 function as control elements for translocation of the mRNA:tRNA complex. *Mol Cell* 12: 321–328
- Datsenko KA, Wanner BL (2000) One-step inactivation of chromosomal genes in *Escherichia coli* K-12 using PCR products. *Proc Natl Acad Sci USA* 97: 6640–6645
- Davis BD (1987) Mechanism of bactericidal action of aminoglycosides. *Microbiol Rev* 51: 341–350
- Davis JH, Williamson JR (2017) Structure and dynamics of bacterial ribosome biogenesis. *Philos Trans R Soc Lond B Biol Sci* 372: 20160181
- De Lay N, Schu DJ, Gottesman S (2013) Bacterial small RNA-based negative regulation: Hfq and its accomplices. *J Biol Chem* 288: 7996–8003
- Del Campo C, Bartholomäus A, Fedyunin I, Ignatova Z (2015) Secondary structure across the bacterial transcriptome reveals versatile roles in mRNA regulation and function. *PLoS Genet* 11: e1005613
- Deutscher MP (2009) Maturation and degradation of ribosomal RNA in bacteria. *Prog Mol Biol Transl Sci* 85: 369–391
- Ellis MJ, Trussler RS, Haniford DB (2015) Hfq binds directly to the ribosome-binding site of IS 10 transposase mRNA to inhibit translation. *Mol Microbiol* 96: 633–650
- Folichon M, Allemand F, Régnier P, Hajnsdorf E (2005) Stimulation of poly(A) synthesis by *Escherichia coli* poly(A) polymerase I is correlated with Hfq binding to poly(A) tails. *FEBS J* 272: 454–463
- Foster C, Champney WS (2008) Characterization of a 30S ribosomal subunit assembly intermediate found in *Escherichia coli* cells growing with neomycin or paromomycin. *Arch Microbiol* 189: 441–449
- Fujii K, Kitabatake M, Sakata T, Ohno M (2012) 40S subunit dissociation and proteasome-dependent RNA degradation in nonfunctional 25S rRNA decay. *EMBO J* 31: 2579–2589
- Hajnsdorf E, Boni IV (2012) Multiple activities of RNA-binding proteins S1 and Hfq. *Biochimie* 94: 1544–1553
- de Haseth PL, Uhlenbeck OC (1980) Interaction of *Escherichia coli* host factor protein with Q beta ribonucleic acid. *Biochemistry* 19: 6146–6151
- Hwang J-Y, Buskirk AR (2017) A ribosome profiling study of mRNA cleavage by the endonuclease RelE. *Nucleic Acids Res* 45: 327–336
- Ingolia NT, Ghaemmaghami S, Newman JRS, Weissman JS (2009) Genome-wide analysis *in vivo* of translation with nucleotide resolution using ribosome profiling. *Science* 324: 218–223
- Jinks-Robertson S, Nomura M (1981) Regulation of ribosomal protein synthesis in an *Escherichia coli* mutant missing ribosomal protein L1. *J Bacteriol* 145: 1445–1447
- Jones PG, Inouye M (1996) RbfA, a 30S ribosomal binding factor, is a cold-shock protein whose absence triggers the cold-shock response. *Mol Microbiol* 21: 1207–1218
- Kaczanowska M, Rydén-Aulin M (2007) Ribosome biogenesis and the translation process in *Escherichia coli*. *Microbiol Mol Biol Rev* 71: 477–494
- Karlsstein K (2013) Quality control mechanisms during ribosome maturation. *Trends Cell Biol* 23: 242–250
- Kufel J, Allmang C, Petfalski E, Beggs J, Tollervey D (2003) Lsm Proteins are required for normal processing and stability of ribosomal RNAs. *J Biol Chem* 278: 2147–2156
- Laursen BS, Sørensen HP, Mortensen KK, Sperling-Petersen HU (2005) Initiation of protein synthesis in bacteria. *Microbiol Mol Biol Rev* 69: 101–123
- Le Derout J, Folichon M, Briani F, Dehò G, Régnier P, Hajnsdorf E (2003) Hfq affects the length and the frequency of short oligo(A) tails at the 3' end of *Escherichia coli* rpsO mRNAs. *Nucleic Acids Res* 31: 4017–4023
- Leong V, Kent M, Jomaa A, Ortega J (2013) *Escherichia coli* rimM and yjeQ null strains accumulate immature 30S subunits of similar structure and protein complement. *RNA* 19: 789–802
- Li G-W, Burkhardt D, Gross C, Weissman JS (2014) Quantifying absolute protein synthesis rates reveals principles underlying allocation of cellular resources. *Cell* 157: 624–635
- Liiv A, Remme J (2004) Importance of transient structures during post-transcriptional refolding of the pre-23S rRNA and ribosomal large subunit assembly. *J Mol Biol* 342: 725–741
- Link TM, Valentin-Hansen P, Brennan RG (2009) Structure of *Escherichia coli* Hfq bound to polyriboadenylate RNA. *Proc Natl Acad Sci USA* 106: 19292–19297
- Lodmell JS, Dahlberg AE (1997) A conformational switch in *Escherichia coli* 16S ribosomal RNA during decoding of messenger RNA. *Science* 277: 1262–1267
- Mikulecky PJ, Kaw MK, Brescia CC, Takach JC, Sledjeski DD, Feig AL (2004) *Escherichia coli* Hfq has distinct interaction surfaces for DsrA, rpoS and poly(A) RNAs. *Nat Struct Mol Biol* 11: 1206–1214
- Mohanty BK, Maples VF, Kushner SR (2004) The Sm-like protein Hfq regulates polyadenylation dependent mRNA decay in *Escherichia coli*. *Mol Microbiol* 54: 905–920
- Moll I, Leitsch D, Steinhauser T, Bläsi U (2003) RNA chaperone activity of the Sm-like Hfq protein. *EMBO Rep* 4: 284–289
- Mortazavi A, Williams BA, McCue K, Schaeffer L, Wold B (2008) Mapping and quantifying mammalian transcriptomes by RNA-Seq. *Nat Methods* 5: 621–628
- Muffler A, Traulsen DD, Fischer D, Lange R, Hengge-Aronis R (1997) The RNA-binding protein HF-I plays a global regulatory role which is largely, but not exclusively, due to its role in expression of the sigmaS subunit of RNA polymerase in *Escherichia coli*. *J Bacteriol* 179: 297–300
- Narla A, Ebert BL (2010) Ribosomopathies: human disorders of ribosome dysfunction. *Blood* 115: 3196–3205
- Nomura M (1999) Regulation of ribosome biosynthesis in *Escherichia coli* and *Saccharomyces cerevisiae*: diversity and common principles. *J Bacteriol* 181: 6857–6864
- O'Connor M, Thomas CL, Zimmermann RA, Dahlberg AE (1997) Decoding fidelity at the ribosomal A and P sites: influence of mutations in three different regions of the decoding domain in 16S rRNA. *Nucleic Acids Res* 25: 1185–1193
- Otaka H, Ishikawa H, Morita T, Aiba H (2011) PolyU tail of rho-independent terminator of bacterial small RNAs is essential for Hfq action. *Proc Natl Acad Sci USA* 108: 13059–13064
- Panja S, Schu DJ, Woodson SA (2013) Conserved arginines on the rim of Hfq catalyze base pair formation and exchange. *Nucleic Acids Res* 41: 7536–7546
- Peng Y, Soper TJ, Woodson SA (2014) Positional effects of AAN motifs in rpoS regulation by sRNAs and Hfq. *J Mol Biol* 426: 275–285
- Powers T, Noller HF (1991) A functional pseudoknot in 16S ribosomal RNA. *EMBO J* 10: 2203–2214

- Régnier P, Hajnsdorf E (2013) The interplay of Hfq, poly(A) polymerase I and exoribonucleases at the 3' ends of RNAs resulting from Rho-independent termination: a tentative model. *RNA Biol* 10: 602–609
- Rochat T, Delumeau O, Figueroa-Bossi N, Noirot P, Bossi L, Dervyn E, Bouloc P (2015) Tracking the elusive function of *Bacillus subtilis* Hfq. *PLoS One* 10: e0124977
- Roy-Chaudhuri B, Kirthi N, Culver GM (2010) Appropriate maturation and folding of 16S rRNA during 30S subunit biogenesis are critical for translational fidelity. *Proc Natl Acad Sci USA* 107: 4567–4572
- Salvail H, Caron M-P, Bélanger J, Massé E (2013) Antagonistic functions between the RNA chaperone Hfq and an sRNA regulate sensitivity to the antibiotic colicin. *EMBO J* 32: 2764–2778
- Sauer E, Weichenrieder O (2011) Structural basis for RNA 3'-end recognition by Hfq. *Proc Natl Acad Sci USA* 108: 13065–13070
- Sauer E, Schmidt S, Weichenrieder O (2012) Small RNA binding to the lateral surface of Hfq hexamers and structural rearrangements upon mRNA target recognition. *Proc Natl Acad Sci USA* 109: 9396–9401
- Scott M, Klumpp S, Mateescu EM, Hwa T (2014) Emergence of robust growth laws from optimal regulation of ribosome synthesis. *Mol Syst Biol* 10: 747
- Shajani Z, Sykes MT, Williamson JR (2011) Assembly of bacterial ribosomes. *Annu Rev Biochem* 80: 501–526
- Shetty S, Varshney U (2016) An evolutionarily conserved element in initiator tRNAs prompts ultimate steps in ribosome maturation. *Proc Natl Acad Sci USA* 113: E6126–E6134
- Sittka A, Lucchini S, Papenfort K, Sharma CM, Rolle K, Binnewies TT, Hinton JCD, Vogel J (2008) Deep sequencing analysis of small noncoding RNA and mRNA targets of the global post-transcriptional regulator, Hfq. *PLoS Genet* 4: e1000163
- Srivastava AK, Schlessinger D (1988) Coregulation of processing and translation: mature 5' termini of *Escherichia coli* 23S ribosomal RNA form in polysomes. *Proc Natl Acad Sci USA* 85: 7144–7148
- Strader MB, Hervey IV WJ, Costantino N, Fujgaki S, Chen CY, Akal-Strader A, Ihunnah CA, Makusky AJ, Court D, Markey SP, Kowalak JA (2013) A coordinated proteomic approach for identifying proteins that interact with the *E. coli* ribosomal protein S12. *J Proteome Res* 12: 1289–1299
- Thurlow B, Davis JH, Leong VF, Moraes T, Williamson JR, Ortega J (2016) Binding properties of YjeQ (RsgA), RbfA, RimM and Era to assembly intermediates of the 30S subunit. *Nucleic Acids Res* 44: 9918–9932
- Tree JJ, Granneman S, McAteer SP, Tollervey D, Gally DL (2014) Identification of bacteriophage-encoded anti-sRNAs in pathogenic *Escherichia coli*. *Mol Cell* 55: 199–213
- Tsui HC, Leung HC, Winkler ME (1994) Characterization of broadly pleiotropic phenotypes caused by an *hfq* insertion mutation in *Escherichia coli* K-12. *Mol Microbiol* 13: 35–49
- Updegrave TB, Zhang A, Storz G (2016) Hfq: the flexible RNA matchmaker. *Curr Opin Microbiol* 30: 133–138
- Vogel J, Luisi BF (2011) Hfq and its constellation of RNA. *Nat Rev Microbiol* 9: 578–589
- Wilusz CJ, Wilusz J (2013) Lsm proteins and Hfq: life at the 3' end. *RNA Biol* 10: 592–601
- Wroblewska Z, Olejniczak M (2016) Hfq assists small RNAs in binding to the coding sequence of *ompD* mRNA and in rearranging its structure. *RNA* 22: 979–994
- Yang Z, Guo Q, Goto S, Chen Y, Li N, Yan K, Zhang Y, Muto A, Deng H, Himeno H, Lei J, Gao N (2014) Structural insights into the assembly of the 30S ribosomal subunit *in vivo*: functional role of S5 and location of the 17S rRNA precursor sequence. *Protein Cell* 5: 394–407
- Yusupov MM, Yusupova GZ, Baucom A, Lieberman K, Earnest TN, Cate JH, Noller HF (2001) Crystal structure of the ribosome at 5.5 Å resolution. *Science* 292: 883–896
- Zhang A, Wassarman KM, Rosenow C, Tjaden BC, Storz G, Gottesman S (2003) Global analysis of small RNA and mRNA targets of Hfq. *Mol Microbiol* 50: 1111–1124
- Zhang A, Schu DJ, Tjaden BC, Storz G, Gottesman S (2013) Mutations in interaction surfaces differentially impact *E. coli* Hfq association with small RNAs and their mRNA targets. *J Mol Biol* 425: 3678–3697
- Ziolkowska K, Derreumaux P, Folichon M, Pellegrini O, Régnier P, Boni IV, Hajnsdorf E (2006) Hfq variant with altered RNA binding functions. *Nucleic Acids Res* 34: 709–720